Drug Design, Development and Therapy

Dovepress
Taylor & Francis Group

Open Access Full Text Article

ORIGINAL RESEARCH

Semaglutide Inhibits Osteoblast Ferroptosis Induced by Diabetic Periodontitis via Modulating the Wnt5a/Ror2/p38 MAPK Signaling Pathway

Zhen Zhang[1], Delong Niu[2], Wenjie Qiu[3], Haoyu Feng[1], Lurong Jia[3], Wenjuan Zhou[3]

[1]School of Stomatology, Binzhou Medical University, Yantai, 264003, People's Republic of China; [2]Department of Stomatology, Lanzhou Petrochemical General Hospital (The Fourth affiliated Hospital of Gansu University of Chinese Medicine), Lanzhou, 730060, People's Republic of China; [3]Department of Oral Implantology, The Affiliated Yantai Stomatological Hospital, Binzhou Medical University, Yantai, 264003, People's Republic of China

Correspondence: Wenjuan Zhou, Email dentzwj@bzmc.edu.cn

Background: Type 2 diabetes mellitus (T2DM) is a major risk factor for periodontitis, often leading to exacerbated alveolar bone loss. Ferroptosis, an iron-dependent regulated cell death pathway, contributes to osteoblast dysfunction under diabetic conditions. The non-canonical Wnt5a/Ror2 pathway is pivotal in inflammation and bone metabolism. Semaglutide, a long-acting GLP-1 receptor agonist, may modulate this pathway and protect osteoblasts from ferroptosis, however, its role in diabetic periodontitis remains unclear.

Methods: MC3T3-E1 osteoblasts were exposed to high glucose plus palmitic acid (HGHP) to mimic a diabetic microenvironment. The effects of Semaglutide on osteoblast proliferation, migration, differentiation, mineralization, and ferroptosis were assessed using EDU, Transwell, ALP and ARS staining, qPCR, Western blotting, ROS, Fe^{2+}, and lipid peroxidation assays. Mechanistic involvement of Wnt5a/Ror2/p38 MAPK signaling was examined using Wnt5a siRNA and a p38 MAPK agonist. In vivo, T2DM mice with ligature-induced periodontitis were treated with semaglutide; alveolar bone and ferroptosis-related markers were assessed by H&E, immunohistochemistry (OPN, GPX4), and 4-HNE immunofluorescence.

Results: HGHP induced osteoblast ferroptosis, increased oxidative stress, and impaired osteogenic function. Semaglutide restored proliferation and osteogenic capacity and attenuated oxidative stress and ferroptosis. Wnt5a was upregulated by HGHP; its silencing reduced ferroptosis and improved osteogenesis. Semaglutide suppressed HGHP-induced Wnt5a/Ror2/p38 MAPK activation, whereas p38 activation blunted its protective effects. In T2DM periodontitis mice, semaglutide reduced periodontal inflammation and osteoblast ferroptosis.

Conclusion: Semaglutide mitigates HGHP-induced osteoblast ferroptosis and improves osteogenic function via the Wnt5a/Ror2/p38 MAPK pathway, supporting its potential in diabetic periodontitis.

Keywords: semaglutide, diabetic periodontitis, ferroptosis, Wnt5a/Ror2, p38 MAPK pathway

Introduction

Type 2 diabetes mellitus (T2DM) is a prevalent metabolic disorder that significantly increases the risk and severity of periodontitis, a chronic inflammatory disease affecting the supporting structures of the teeth. Patients with diabetic periodontitis often exhibit accelerated alveolar bone loss compared to non-diabetic individuals, which contributes to tooth mobility and eventual tooth loss.[1,2] The underlying mechanisms linking hyperglycemia to impaired bone homeostasis remain incompletely understood, but increasing evidence indicates that regulated forms of cell death play a central role in this process.

Ferroptosis is a recently characterized, iron-dependent form of regulated cell death driven by lipid peroxidation. Unlike apoptosis or necrosis, ferroptosis is closely associated with iron metabolism and reactive oxygen species (ROS) accumulation.[3,4] Emerging evidence has implicated ferroptosis in periodontal tissue injury. For example, fibroblast ferroptosis has been reported to contribute to periodontitis-induced tissue damage and alveolar bone loss.[5] In addition, accumulating studies suggest that ferroptosis may contribute to osteoblast dysfunction under pathological conditions,

https://doi.org/10.2147/DDDT.S599539
Received: 2 March 2026
Accepted: 8 May 2026
Published: 22 May 2026

including hyperglycemia and chronic inflammation.[6–12] Given that osteoblasts are essential for bone formation and mineralization, dysregulation of ferroptosis could exacerbate alveolar bone loss in diabetic periodontitis.

The Wnt signaling pathway is a critical regulator of bone metabolism. In particular, the non-canonical Wnt5a/Ror2 pathway modulates osteoblast differentiation, inflammatory responses, and oxidative stress.[13–16] Dysregulation of Wnt5a/Ror2 signaling has been implicated in impaired bone formation and inflammatory bone diseases. However, whether this pathway mediates ferroptosis in osteoblasts under diabetic conditions has not been fully elucidated.

Glucagon-like peptide-1 (GLP-1) receptor agonists, including Semaglutide, are widely used for glycemic control in T2DM and have demonstrated beneficial effects beyond glucose regulation, such as anti-inflammatory and cardioprotective actions.[17–20] Recent studies indicate that GLP-1 receptor signaling can influence osteogenic differentiation and bone metabolism.[21–23] These findings raise the possibility that Semaglutide may exert protective effects on osteoblasts by modulating ferroptosis, potentially via Wnt5a/Ror2-mediated signaling.[17–23]

In this study, we aimed to investigate whether Semaglutide could inhibit ferroptosis in osteoblasts under a high-glucose, high-lipid environment mimicking diabetic conditions, and to elucidate the underlying mechanisms involving the Wnt5a/Ror2/p38 MAPK signaling pathway. Furthermore, we sought to assess the therapeutic potential of Semaglutide in preventing alveolar bone loss in a mouse model of diabetic periodontitis.

Materials and Methods

Cell Culture

MC3T3-E1 pre-osteoblasts were obtained from (BNCC, Henan, China) and cultured in α-Minimum Essential Medium (α-MEM; Gibco, USA) supplemented with 10% fetal bovine serum (FBS; Gibco, USA) and 1% penicillin-streptomycin (P/S; Solarbio, Beijing, China). Cells were maintained at 37°C in a humidified atmosphere containing 5% CO_2. To mimic the diabetic microenvironment, cells were exposed to high-glucose (30 mM) and palmitic acid (0.2mM) culture medium.[24] Semaglutide (MCE, USA) was dissolved in DMSO and administered at various concentrations (eg., 10, 50, 100 μM) for 24 hours. Ferroptosis was modulated using Ferrostatin-1 (Fer-1; a ferroptosis inhibitor). For pathway intervention experiments, cells were transfected with Wnt5a siRNA to knock down Wnt5a expression or pretreated with Anisomycin (MCE, USA), a p38 MAPK activator, prior to Semaglutide exposure, to evaluate the involvement of the Wnt5a/Ror2/p38 MAPK signaling pathway in HGHP-induced osteoblast ferroptosis and osteogenic dysfunction.

Cell Viability Assay (CCK-8)

Cell viability was determined using a Cell Counting Kit-8 (CCK-8; Dojindo, Japan). MC3T3-E1 cells were seeded into 96-well plates at a density of 5×10^3 cells/well and treated with Semaglutide under high-glucose conditions for 24 or 48 hours. Subsequently, 10 μL of CCK-8 reagent was added to each well and incubated for 2 hours at 37°C. The absorbance was measured at 450 nm using a microplate reader (BioTek, USA). Results were expressed as a percentage of control.

Transwell Migration Assay

Transwell assays were performed using 8 μm pore-size chambers (Corning, USA). Cells (5×10^4 per well) suspended in serum-free medium were seeded into the upper chamber, while the lower chamber contained medium with 10% FBS. After incubation for 24 hours, non-migrated cells were removed, and migrated cells on the lower surface were fixed with 4% paraformaldehyde and stained with 0.1% crystal violet. Images were taken in five random fields under a light microscope, and the number of migrated cells was quantified using ImageJ.

Osteogenic Differentiation and Mineralization

Cells were seeded into 24-well plates (Jet Biofil) at a density of 2×10^4cells per well (counted with Countstar, IE1000, China) and cultured in osteogenic medium containing 10% FBS, 10 nmol/L dexamethasone, 10 mmol/L β-Glycerophosphate disodium salt pentahydrate and 50 μg/mL vitamin C.[25] Osteogenic differentiation and mineralization were evaluated on day7 and 14 using the BCIP/NBT Alkaline Phosphatase Color Development Kit (C3206, Beyotime) and Alizarin Red

S Solution (ALIR-10001, cyagen). HGHP is continuously maintained in the induction medium to mimic the chronic progression of diabetes.

Detection of Reactive Oxygen Species (ROS)

Intracellular ROS levels were detected using a DCFH-DA fluorescent probe (Beyotime, China). Cells were incubated with 10 μM DCFH-DA at 37°C for 30 minutes in the dark, then washed twice with PBS followed by immediate analysis under the microscope.

Lipid Peroxidation and Iron Assays

Lipid peroxidation was assessed by lipid peroxidation assay kit BODIPY 581/591 C11 (Beyotime, China). Cellular ferrous iron (Fe^{2+}) levels were quantified using an FerroOrange (Dojindo, Japan). According to the manufacturer's instructions, cells were incubated with 1 μmol/L probes for 30 min at 37 °C in the dark. Subsequently, the cells were rinsed with balanced salt solution. The images were captured using an microscope and analyzed by Image J.

Transmission Electron Microscopy (TEM)

Fresh cell samples were fixed in 2.5% glutaraldehyde (sigma-Aldrich, G5882) at 4 °C for 24 h, followed by three washes with PBS. The specimens were then post-fixed with 1% osmium tetroxide, dehydrated, and embedded. Subsequently, the samples were sectioned into 70–90 nm utilizing a LEICA EM UC7 ultramicrotome. These sections were stained with a combination of lead citrate and uranyl acetate. Finally, the mitochondrial ultrastructural changes were visualized using a HITACHI HT7700 transmission electron microscope.

Quantitative Real-Time PCR (RT-qPCR)

Total RNA was extracted from MC3T3-E1 cells using TRIzol reagent (Invitrogen, USA) according to the manufacturer's protocol. RNA purity and concentration were determined using a NanoDrop 2000 spectrophotometer (Thermo Fisher Scientific, USA). cDNA was synthesized using the PrimeScript RT reagent kit (Takara, Japan). Quantitative real-time PCR was performed using SYBR Premix Ex Taq II (Takara, Japan) on a QuantStudio 6 Flex Real-Time PCR System (Applied Biosystems, USA). Actb served as the internal control, and relative mRNA expression was calculated using the $2^{-\Delta\Delta Ct}$ method. The primer sequences used were detailed in Table 1.

Western Blotting

Proteins were extracted from MC3T3-E1 cells and mouse alveolar bone tissues using RIPA lysis buffer (Beyotime Biotechnology, Shanghai, China) containing protease and phosphatase inhibitors (Sangon Biotech, Shanghai, China).

Table 1 Primers for Quantitative Real-Time Polymerase Chain Reaction (qPCR)

Gene	Forward (5′→3′)	Reverse (5′→3′)
ALP	GTTGCCAAGCTGGGAAGAAC	GCTGCTGAGTGACACAGGAA
RUNX2	CCTGAACTCTGCACCAAGTC	TGGCTTCCAGATGTTCTCTG
OCN	AGCAAAGGTGCAGCCTTTGT	GCGCCTGGGTCTCTTCACT
COL1A1	GCTCCTCTTAGGGGCCACT	CCACGTCTCACCATTGGGG
Wnt5a	GAGTGCCCGAGTGAAAGTGA	CTTCTGCTTCACACCTTGGG
Wnt11	CTCAGCTACGGGCTCCTCA	ATGGCATTTACACTTCGTTTCC
Ror2	GCCTGGTGGGATGAGGAACT	TCCCTGTCCAAAGCAGAGGA
JUN	TGGGCACATCACCACTACAC	TCTGGCTATGCAGTTCAGCC
MAPK9	CGGACTCAACTTTCACTG	TAAGAGGACGAGTTCACG
GPX4	AGGACATCGACGTGGTGAC	GCTCAGGTAGCGACGAGGAA
SLC7A11	TCCAGAGGACACTGCCAAAG	ATCGGAGACCAACAGGCTGA
ACSL4	TGACGACCAAGACCTGTTCC	GGTCTTGTCACGGTGGACTG
β-actin	CACTGTCGAGTCGCGTCC	TCATCCATGGCGAACTGGTG

https://doi.org/10.2147/DDDT.S599539

Protein concentrations were determined using the BCA Protein Assay Kit (Beyotime Biotechnology, Shanghai, China). Equal amounts of proteins were separated by SDS–PAGE and transferred onto PVDF membranes (Biosharp, Beijing, China). Membranes were blocked with 5% non-fat milk for 1 h at room temperature and incubated overnight at 4°C with the following primary antibodies: anti-Wnt5a (1:1000, Invitrogen, PA5-88735), anti-Ror2 (1:1000, Invitrogen, PA5-102946), anti-p38 MAPK (1:1000, Cell Signaling Technology, 9212S), anti-phospho-p38 MAPK (1:1000, Cell Signaling Technology, 4511S), anti-GPX4 (1:5000, Abcam, ab125066), anti-SLC7A11 (1:2000, Proteintech, 26864-1-AP), anti-ACSL4 (1:10000, Abcam, ab155282), anti-β-actin (1:4000, Proteintech, 20536-1-AP). After washing, membranes were incubated with HRP-conjugated goat anti-rabbit or anti-mouse secondary antibodies (Beyotime Biotechnology, Shanghai, China) for 1 h at room temperature. Protein bands were visualized using an ECL detection kit (Beyotime Biotechnology) and analyzed by Image J software.

Immunofluorescence Staining

MC3T3-E1 cells were seeded on glass coverslips in 24-well plates and treated as indicated. Cells were fixed with 4% paraformaldehyde for 15 min, permeabilized with 0.1% Triton X-100 for 10 min, and blocked with 5% bovine serum albumin (BSA) for 1 h. Cells were then incubated overnight at 4°C with primary antibodies: anti-Wnt5a (Abcam, ab174963), anti-Ror2 (Proteintech, 12472-1-AP). After washing, cells were incubated with Alexa Fluor 488– or 594–conjugated secondary antibodies (Invitrogen, USA) for 1 h at room temperature and counterstained with DAPI (Beyotime, China). Images were captured using a confocal laser scanning microscope (Leica TCS SP8, Germany).

RNA Sequencing and Bioinformatic Analysis

Transcriptome sequencing was conducted for cell RNA samples obtained from the control, HGHP and HGHP+SEMA. Each group consisted of five independent biological replicates. The total RNA was extracted and sequenced utilizing an Illumina Novaseq platform by Honsunbio Technology Co., Ltd (Shanghai, China). Differential expression analysis was performed between groups using normalized gene expression counts. Differentially expressed genes (DEGs) were screened using the criteria of $|\log2 \text{ fold change}| > 1$ and false discovery rate (FDR) < 0.05. Multiple testing correction was performed using the Benjamini–Hochberg method. GO and KEGG enrichment analyses of DEGs were performed using BioLadder (BioLadder.cn), and enriched terms or pathways with $P < 0.05$ were considered statistically significant.

Animal Experiments

All animal experiment conducted in this study were complied with the guidelines of the Committee on the Use and Care of Animal of the Binzhou Medical University (Yantai, Shandong). Five-week-old mice were purchased from GemPharmatech Co., Ltd and housed in individually ventilated cages under specific pathogen-free conditions. The mice were provided sterile feed and maintained under a 12 h light/dark cycle, with the room temperature controlled at 24 ± 2 °C and relative humidity regulated within the range of (55 ± 5)%.

Mice were maintained under pathogen-free conditions and allowed to acclimate for one week before being fed a high fat/high glucose diet (HFHG, D12492, Research Diets, USA). After 4 weeks of feeding, the mice reached a body weight of 32 to 38g and were intraperitoneally injected with streptozotocin (STZ, 40 mg/kg, S0130, Sigma, USA) for 5 consecutive days. One week after the last injection, the relevant parameters were measured. Mice with fasting plasma glucose levels higher than 16.7 mM and clinical symptoms of increased food and water consumption, increased urine output, and weight loss were diagnosed with T2DM.

Experimental periodontitis model: After mice were anesthetized by intraperitoneal injection of 1% sodium pentobarbital solution (50mg/kg, Notlas, China), 4–0 wire ligature was inserted between the maxillary first and second molars, with both sides knoted, and left in place for 14 days. Check for loose or displaced ligations every two days and insert new ligations immediately if they come off. Animal group allocation: Successfully modeled T2DM mice were randomly divided into four groups (n = 6):

1. Only diabetic group;
2. Diabetes with periodontitis (DP) group (ligation-induced experimental periodontitis for 14 days);

3. DP+somalutide group (somalutide treated experimental diabetic periodontitis once a day in the morning for 14 days).
4. DP+Fer-1(ferroptosis inhibitor) treated experimental diabetic periodontitis once daily in the morning for 14 days. Thus, the overall animal experiment included five groups: Control, T2DM, DP, DP + SEMA, and DP + Fer-1.

Based on previous studies using similar diabetic periodontitis mouse models and in accordance with the principle of minimizing animal use, six mice were included in each group. After successful establishment of the T2DM model, mice were randomly assigned to the experimental groups. Outcome assessments, including histological evaluation, and immunohistochemical quantification, were performed by investigators blinded to the group allocation.

Histological and Immunohistochemical Staining

Mouse maxillae were fixed in 4% paraformaldehyde, decalcified in 10% EDTA for 4 weeks, dehydrated, and embedded in paraffin. Sections (5 μm) were subjected to hematoxylin and eosin (H&E). For immunohistochemistry, sections were deparaffinized, rehydrated, and subjected to antigen retrieval in citrate buffer (pH 6.0). Endogenous peroxidase activity was blocked with 3% H_2O_2, followed by 5% BSA blocking for 30 min. Sections were then incubated overnight at 4°C with primary antibodies against: GPX4 (Abcam, ab125066) and OPN (Proteintech, 22952-1-AP). After washing, sections were incubated with HRP-conjugated secondary antibodies (Servicebio, China) and developed using DAB substrate (ZSGB-BIO, Beijing, China). Counterstaining was performed with hematoxylin. Stained sections were examined and photographed under a light microscope (Olympus BX53, Japan).

Ethical Statement

All animal experiments were approved by the Institutional Animal Care and Use Committee of Binzhou Medical University under protocol number (2024-L081). All procedures complied with the National Institutes of Health guidelines for the care and use of laboratory animals. At the end of the experiment, mice were euthanized by carbon dioxide asphyxiation in accordance with the AVMA Guidelines for the Euthanasia of Animals, and tissues were collected for histology.

Statistical Analysis

Data were expressed as mean ± standard deviation (SD) from at least five independent experiments. Statistical analyses were performed using GraphPad Prism 10.0 software (GraphPad Software, USA). Comparisons between two groups were conducted using Student's *t*-test, while multiple groups were analyzed by one-way ANOVA followed by Tukey's post hoc test. Statistical significance was defined as $p < 0.05$.

Results

High-Glucose and High-Palmitic (HGHP) Induce Ferroptosis of MC3T3-E1 Cells in vitro

To identify whether ferroptosis was activated in HGHP-treated cells, MC3T3-E1 cells were first exposed to HGHP, and intracellular ROS levels were detected using DCFH-DA staining. Compared with the control group, HGHP exposure led to marked oxidative stress and ferroptotic responses. As shown in Figure 1A–D, DCFH-DA and BODIPY staining revealed a significant increase in intracellular total ROS and lipid ROS levels, accompanied by enhanced Fe^{2+} fluorescence intensity. Quantitative analyses further confirmed that HGHP conditions markedly elevated intracellular Fe^{2+} accumulation and ROS intensity, indicating the induction of ferroptosis-like oxidative injury. Next, we evaluated whether HGHP stress affected osteoblast proliferation and migration. EdU incorporation assays showed that the proportion of proliferating MC3T3-E1 cells was significantly decreased following HGHP treatment (Figure 1E–H). Similarly, transwell migration assays demonstrated a pronounced reduction in cell motility under HGHP conditions (Figure 1F–H). In addition, osteogenic differentiation was examined by ALP staining at day 7 and Alizarin Red S staining at day 14. Both ALP activity and calcium nodule formation were markedly suppressed in HGHP-treated cells (Figure 1G), suggesting impaired osteogenic potential.

Collectively, these findings demonstrate that high-glucose and high-palmitate exposure induces excessive ROS generation and Fe^{2+} accumulation, promoting ferroptosis and leading to osteogenic dysfunction in MC3T3-E1 cells.

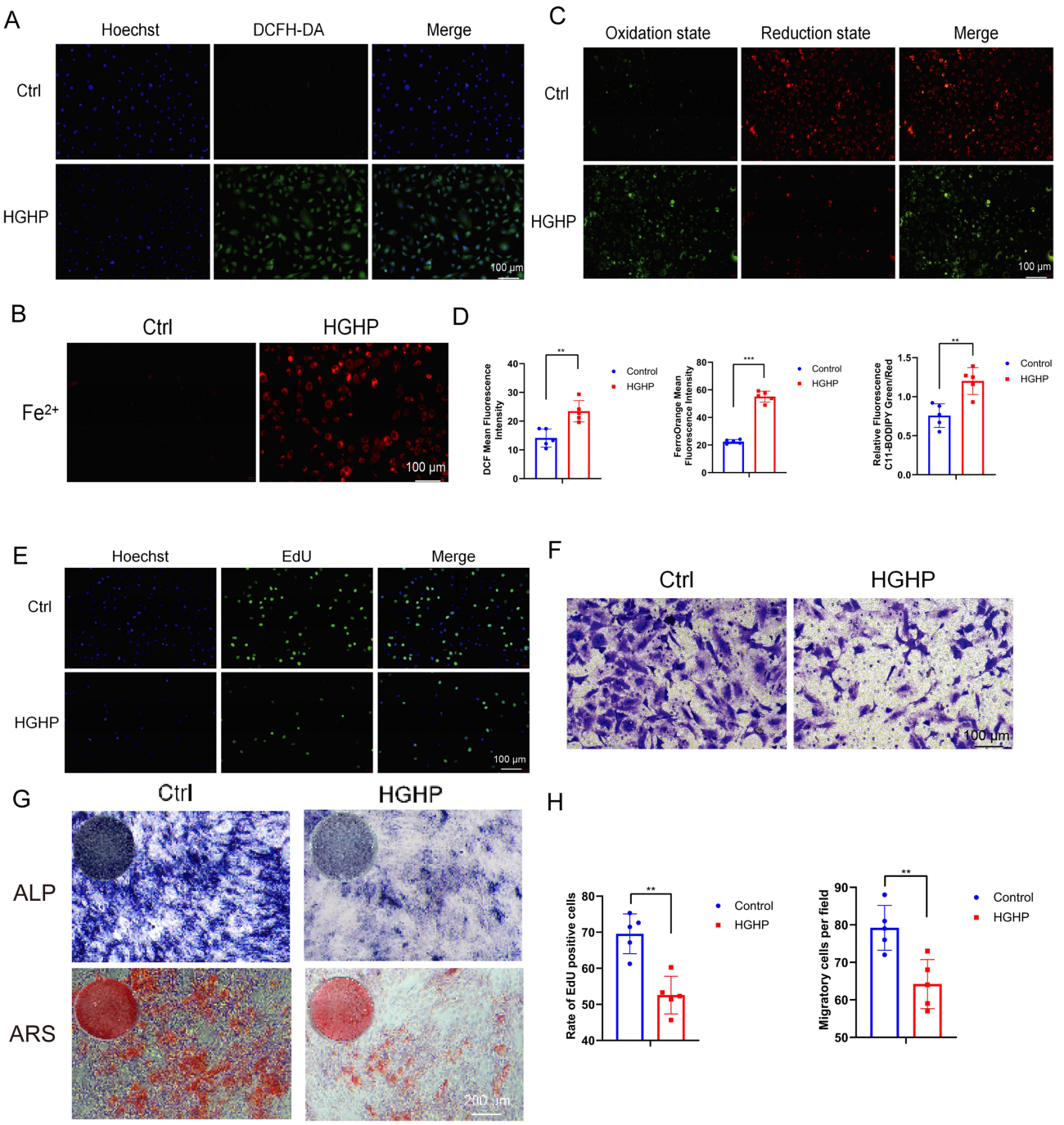

Figure 1 High-glucose and high-palmitate (HGHP) treatment induces ferroptosis and suppresses osteogenic function in MC3T3-E1 cells (**A**) DCFH-DA staining showing intracellular ROS accumulation in control and HGHP-treated cells. (**B**) Fe^{2+} fluorescence staining indicating intracellular iron overload after 48 h HGHP exposure. (**C**) Lipid ROS staining visualizing lipid peroxidation levels. (**D**) Quantitative analysis of ROS, Fe^{2+}, and lipid ROS fluorescence intensity. (**E**) Representative EdU staining showing proliferating cells (green) and nuclei (blue).(**F**) Representative transwell images showing migrated MC3T3-E1 cells after HGHP treatment. (**G**) ALP staining (day 7) and Alizarin Red S staining (day 14) showing osteogenic differentiation and mineralization capacity. (**H**) Quantification of EdU-positive cells and migrated cell number. Data are presented as mean ± SD (n = 5). $^{**}p < 0.01$, $^{***}p < 0.001$. Scale bars = 100 μm.

Semaglutide Alleviates HGHP-Induced Osteogenic Impairment and Ferroptosis in MC3T3-E1 Cells

Semaglutide (SEMA), a long-acting GLP-1 receptor agonist, has been reported to exert anti-inflammatory and cytoprotective activities beyond glycemic regulation. To determine whether SEMA mitigates high glucose and high palmitate

https://doi.org/10.2147/DDDT.S599539

(HGHP)-induced osteogenic dysfunction, we first assessed its cytotoxicity and optimal working concentration. CCK-8 assay showed that SEMA displayed no cytotoxicity to MC3T3-E1 cells up to 40 μM, while 10 μM significantly improved cell viability under HGHP conditions; therefore, 10 μM was selected for subsequent experiments (Figure 2A and B).

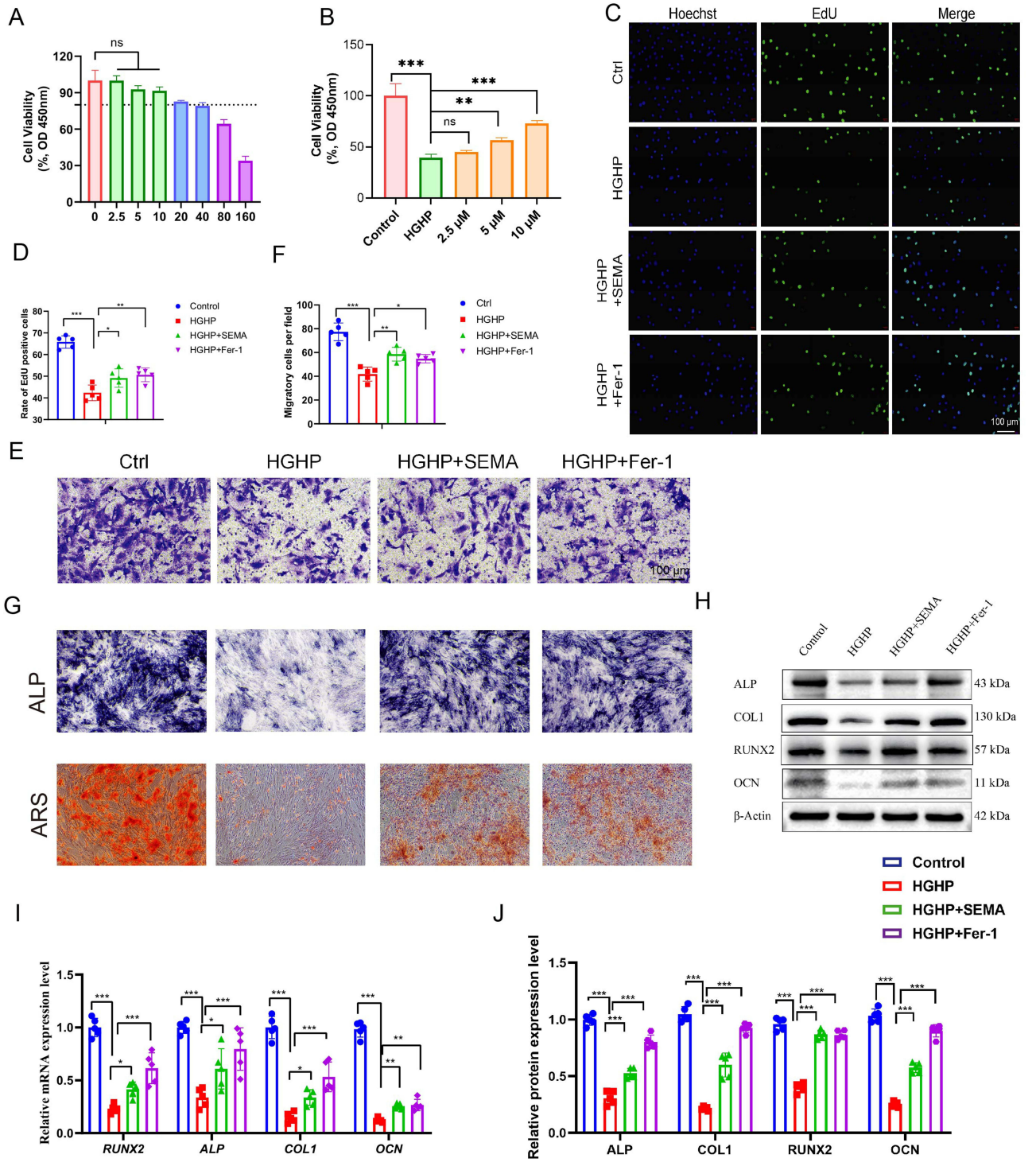

Figure 2 Semaglutide restores proliferation, migration, and osteogenic function of MC3T3-E1 cells under HGHP conditions. (**A**) CCK-8 cytotoxicity assay of SEMA at different concentrations. (**B**) Determination of the optimal working concentration showing maximal viability improvement at 10 μM. (**C** and **D**) Representative EdU fluorescence images and quantification showing that SEMA or Fer-1 significantly enhanced proliferation compared with HGHP. (**E** and **F**) Representative transwell migration images and quantification showing increased cell migration following SEMA or Fer-1 treatment. (**G**) ALP and ARS staining after 7 and 14 days of osteogenic induction demonstrating restored differentiation and mineralization with SEMA or Fer-1. (**H–J**) RT-qPCR and Western blot analyses showing expression and densitometric quantification of osteogenic markers (RUNX2, ALP, COL1, OCN) in each group. Data are presented as mean ± SD (n = 5). **p* < *0.05*, ***p* < *0.01*, ****p* < *0.001*. Scale bars = 100μm.

https://doi.org/10.2147/DDDT.S599539

Compared with the HGHP group, both SEMA and the ferroptosis inhibitor Fer-1 significantly promoted cell proliferation and migration, as revealed by EdU incorporation assays (Figure 2C) and transwell migration assays (Figure 2D). Quantitative analyses of proliferation and migration are shown in Figure 2E and F, respectively. ALP and Alizarin Red S (ARS) staining after 7 and 14 days of osteogenic induction further demonstrated that SEMA treatment markedly restored osteogenic differentiation and matrix mineralization suppressed by HGHP stimulation (Figure 2G). Consistently, RT-qPCR and Western blot analyses revealed that the mRNA and protein expression levels of osteogenic markers—RUNX2, ALP, COL1, and OCN—were significantly downregulated in the HGHP group but recovered after SEMA or Fer-1 administration (Figure 2H–J).

To explore whether the protective effects of SEMA were related to ferroptosis inhibition, ferroptosis-associated parameters were next evaluated. Fluorescence staining showed that SEMA significantly reduced intracellular Fe^{2+} accumulation, ROS, and lipid ROS levels induced by HGHP (Figure 3A–E). In parallel, HGHP exposure markedly decreased the expression of GPX4 and SLC7A11, key regulators of lipid peroxide detoxification, while SEMA treatment restored their levels to near-control values (Figure 3F and G). Transmission electron microscopy further revealed that HGHP treatment caused characteristic ferroptotic mitochondrial damage, including condensed membranes and diminished cristae, which was markedly alleviated by SEMA (Figure 3H).

Collectively, these findings demonstrate that semaglutide alleviates HGHP-induced osteogenic impairment by suppressing oxidative stress and ferroptosis, likely through restoration of GPX4/SLC7A11-mediated redox homeostasis.

Semaglutide Suppresses Aberrant Activation of the Wnt5a/Ror2/p38 MAPK Signaling Pathway Under HGHP Conditions

To elucidate the molecular mechanism underlying the protective effects of semaglutide (SEMA) against HGHP-induced osteogenic injury and ferroptosis, we performed transcriptomic profiling of MC3T3-E1 cells in the control, HGHP, and HGHP +SEMA groups. Venn diagram analysis identified a distinct subset of differentially expressed genes (DEGs) that were specifically altered by HGHP stimulation and reversed upon SEMA treatment (Figure 4A). Pathway enrichment analysis revealed that genes differentially expressed in the HGHP group were predominantly enriched in ferroptosis, oxidative stress, and non-canonical Wnt signaling pathways. In contrast, after SEMA administration, enrichment in ferroptosis- and inflammation-related pathways was markedly reduced, whereas pathways associated with metabolic regulation and osteogenic differentiation were enhanced (Figure 4B). Consistent with these findings, GO enrichment analysis demonstrated that biological processes including "oxidative stress response," "regulation of cell death," and "MAPK cascade" were significantly activated under HGHP conditions but attenuated after SEMA intervention (Figure 4C). Given the prominent involvement of the Wnt signaling pathway in the enriched terms, we next focused on the non-canonical Wnt5a/Ror2/p38 MAPK axis. RT-qPCR analysis showed that HGHP stimulation significantly upregulated mRNA expression levels of Wnt5a, Ror2, Dvl2, Jun, p38, and MAPK9, whereas SEMA treatment substantially reduced their expression (Figure 4D). Consistent with transcriptional changes, Western blot analysis confirmed increased protein expression of Wnt5a, Ror2, Dvl2, Jun, and phosphorylated p38 in the HGHP group, all of which were restored toward control levels following SEMA treatment (Figure 4E and F).

Collectively, these results indicate that exposure to high-glucose and high-palmitate conditions aberrantly activates the Wnt5a/Ror2/p38 MAPK signaling pathway, contributing to oxidative stress and ferroptotic injury in osteoblasts. Semaglutide effectively suppresses this overactivation, thereby restoring redox balance and promoting osteogenic recovery under diabetic metabolic stress.

Silencing of Wnt5a Attenuates HGHP-Induced Ferroptosis and Enhances Osteogenic Differentiation

To verify the involvement of Wnt5a in HGHP-induced ferroptosis and osteogenic dysfunction, Wnt5a expression was silenced using specific small interfering RNA (siWNT5a). The knockdown efficiency was confirmed by RT-qPCR (Figure 5C). Immunofluorescence co-localization revealed strong cytoplasmic and membranous overlap of Wnt5a and its receptor Ror2 in osteoblasts under HGHP conditions, whereas siWNT5a treatment markedly decreased the fluorescence intensity of both proteins (Figure 5J), indicating successful inhibition of the Wnt5a/Ror2 signaling complex.

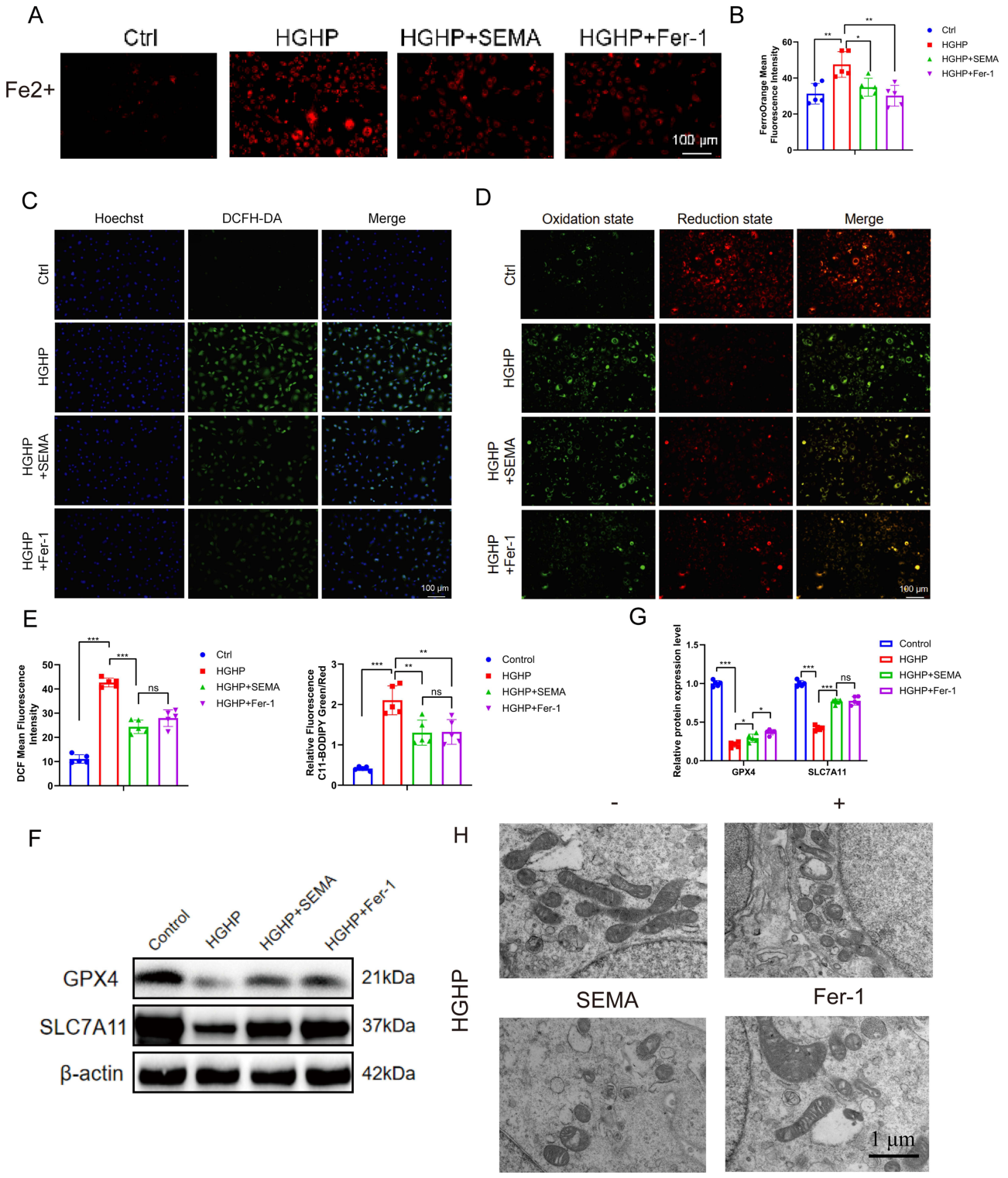

Figure 3 Semaglutide attenuates ferroptosis and oxidative stress induced by HGHP exposure. (**A** and **B**) Fe^{2+} fluorescence staining and quantitative analysis of intracellular iron accumulation. (**C**) DCFH-DA staining of intracellular ROS production. (**D**) Lipid ROS probe staining showing lipid peroxidation. (**E**) Quantitative analysis of intracellular ROS (left) and lipid ROS levels (right).(**F**) Western blot analysis of GPX4 and SLC7A11 expression in each group. (**G**) Densitometric quantification of GPX4 and SLC7A11 protein levels. (**H**) Transmission electron microscopy showing mitochondrial morphology changes, including condensed membranes and loss of cristae in HGHP-treated cells, which were restored by SEMA treatment. Data are presented as mean ± SD (n = 5). **P < 0.05, **P < 0.01, ***P < 0.001, ns >0.05*. Scale bars = 100 μm.

https://doi.org/10.2147/DDDT.S599539

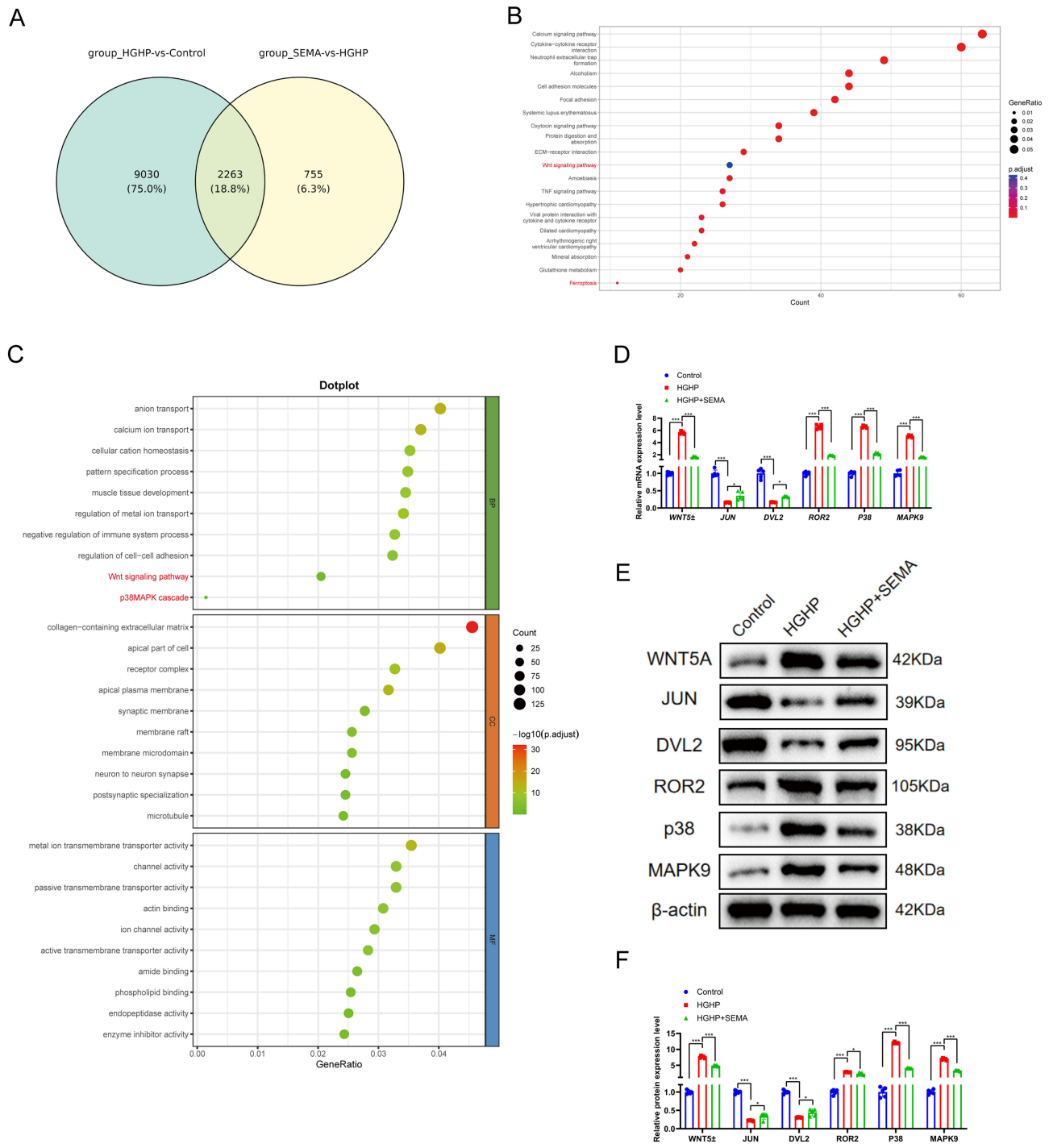

Figure 4 Semaglutide suppresses aberrant activation of the Wnt5a/Ror2/p38 MAPK signaling pathway under HGHP conditions. (**A**) Venn diagram showing the overlap of differentially expressed genes (DEGs) among control, HGHP, and HGHP+SEMA groups. (**B**) KEGG enrichment analysis between control and HGHP groups showing significant enrichment of ferroptosis, oxidative stress, and Wnt signaling pathways. (**C**) GO enrichment analyses displaying biological processes associated with oxidative stress response, regulation of cell death, and MAPK cascade activation under HGHP exposure and their attenuation following SEMA treatment. (**D**) RT-qPCR validation showing relative mRNA expression levels of Wnt5a, Ror2, Dvl2, Jun, p38, and MAPK9 in each group. (**E**) Western blot analysis and densitometric quantification of Wnt5a, Ror2, Dvl2, Jun, and p38/MAPK9 protein expression. (**F**) Densitometric quantification of Wnt5a, Ror2, Dvl2, Jun, and p38/MAPK9 protein expression. Data are presented as mean ± SD (n = 5). *$p < 0.05$, **$p < 0.01$, **$p < 0.001$.

Functionally, suppression of Wnt5a significantly improved osteogenic capacity impaired by HGHP exposure. ALP staining (day 7) and Alizarin Red S (ARS) staining (day 14) demonstrated enhanced alkaline phosphatase activity and increased mineralized nodule formation in the HGHP+siWNT5a group compared with the HGHP+siNC group

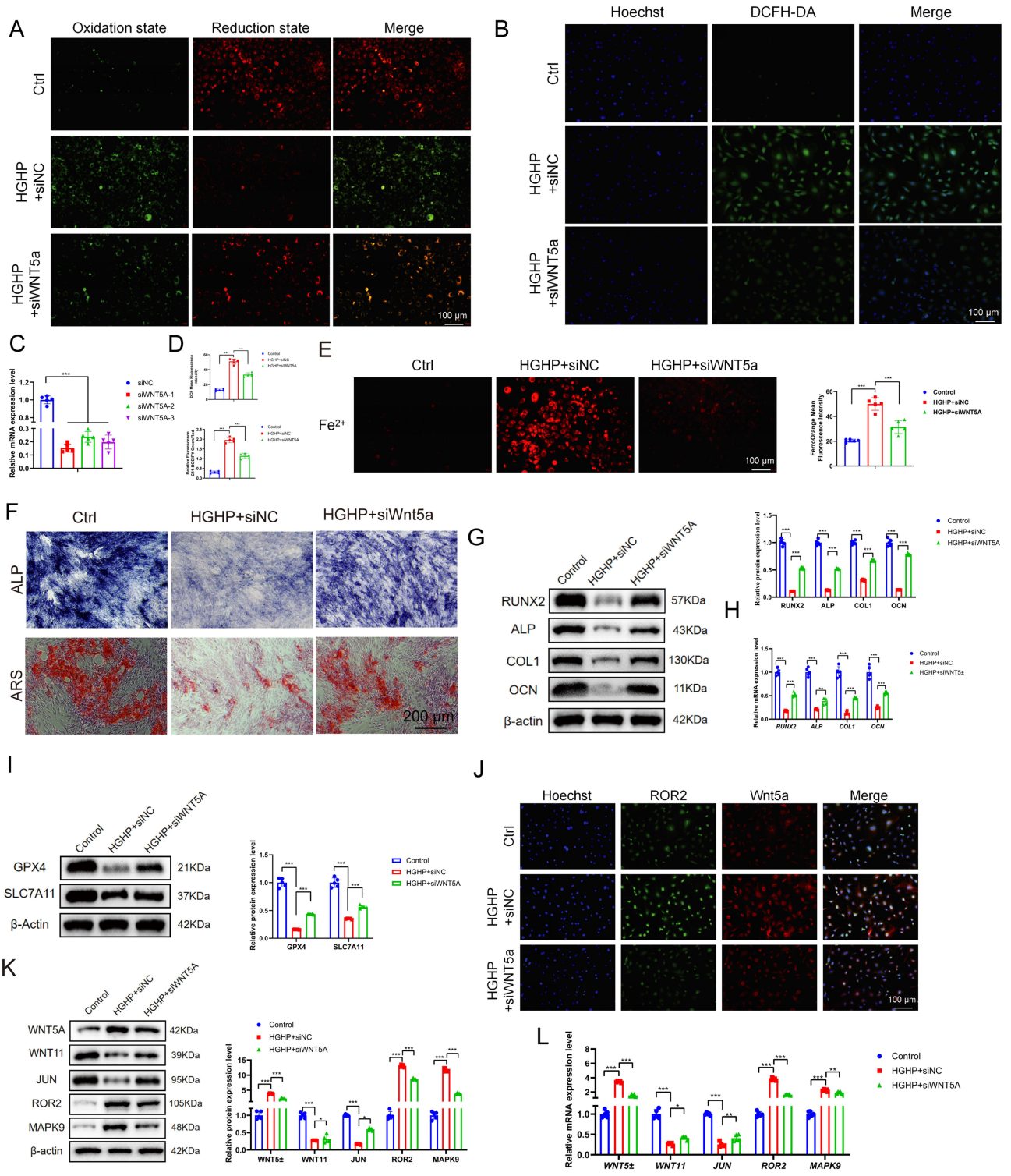

Figure 5 Silencing of Wnt5a attenuates HGHP-induced ferroptosis and restores osteogenic differentiation of osteoblasts.(**A**) Lipid ROS fluorescence staining in osteoblasts. (**B**) Total ROS levels detected by DCFH-DA staining. (**C**) Knockdown efficiency of Wnt5a confirmed by qPCR. (**D**) Quantitative analysis of lipid ROS and total ROS levels. (**E**) Fe^{2+} fluorescence staining and quantification of intracellular iron accumulation. (**F**) ALP staining (day 7) showing osteogenic differentiation and Alizarin Red S (ARS) staining (day 14) showing mineralization capacity.(**G**) Western blot analysis of osteogenic marker proteins and quantification of (RUNX2, ALP, COL1, OCN). (**H**) RT-qPCR analysis of osteogenic genes (RUNX2, ALP, COL1, OCN). (**I**) Western blot analysis of ferroptosis-related proteins GPX4 and SLC7A11. (**J**) Immunofluorescence co-localization of Wnt5a (red) and Ror2 (green). (**K**) Western blot analysis of Wnt5a/Ror2/p38 MAPK pathway-related proteins and quantification of protein expression.(**L**) RT-qPCR analysis of Wnt5a/Ror2/p38 MAPK pathway-related genes.Data are presented as mean ± SD (n = 5). *$P < 0.05$, **$P < 0.01$, ***$P < 0.001$. Scale bars = 100 μm.

https://doi.org/10.2147/DDDT.S599539

(Figure 5F). Consistently, both RT-qPCR and Western blot analyses showed upregulated expression of osteogenic markers RUNX2, ALP, COL1, and OCN following Wnt5a knockdown (Figure 5G and H). Next, ferroptosis-associated oxidative damage was assessed. Compared with HGHP+siNC, the HGHP+siWNT5a group exhibited markedly reduced intracellular lipid ROS, total ROS, and Fe^{2+} accumulation (Figure 5A–E). Western blot analysis further revealed increased expression of ferroptosis-protective proteins GPX4 and SLC7A11 after Wnt5a silencing (Figure 5I), indicating suppression of ferroptotic injury. At the signaling level, both transcriptional and protein analyses confirmed that silencing Wnt5a downregulated key components of the noncanonical Wnt5a/Ror2–MAPK9 pathway, including WNT5a, WNT11, JUN, ROR2, and MAPK9 (Figure 5K and L).

Collectively, these findings demonstrate that Wnt5a silencing mitigates HGHP-induced ferroptosis and oxidative stress while restoring osteogenic differentiation, largely through inhibition of the Wnt5a/Ror2–MAPK9 signaling cascade.

Wnt5a is Essential for the Protective Effects of Semaglutide Against Ferroptosis and Osteogenic Dysfunction

To further determine whether Wnt5a is a critical mediator of semaglutide (SEMA)–induced cytoprotection, we silenced Wnt5a in osteoblasts exposed to HGHP conditions in the presence of semaglutide. Western blot analysis demonstrated that semaglutide markedly decreased Wnt5a expression compared with the HGHP group, and this reduction was further enhanced by siWnt5a transfection (Figure 6A).

Functionally, semaglutide treatment significantly improved osteogenic differentiation and mineralization potential under HGHP stimulation, as evidenced by intensified alkaline phosphatase (ALP) activity and enhanced calcium nodule formation at both 7 and 14 days (Figure 6C). However, these restorative effects were further enhanced when Wnt5a was silenced, indicating that inhibition of Wnt5a contributes to the pro-osteogenic action of Semaglutide. Consistent with these observations, RT-qPCR and Western blot analyses revealed increased expression of osteogenic markers RUNX2, ALP, COL1, and OCN in the HGHP + SEMA + siNC group, and these increases were further enhanced in the HGHP + SEMA + siWnt5a group (Figure 6B–I). In addition, Semaglutide markedly alleviated HGHP-induced ferroptosis, as shown by restored expression of the ferroptosis-protective proteins GPX4 and SLC7A11 (Figure 6F and G). Wnt5a knockdown further increased GPX4 and SLC7A11 expression in the presence of Semaglutide. Furthermore, fluorescence staining revealed that Semaglutide significantly reduced lipid ROS accumulation in osteoblasts, and this reduction was further strengthened by Wnt5a knockdown (Figure 6D and E).

Collectively, these findings demonstrate that Wnt5a inhibition further enhances the protective effects of Semaglutide against HGHP-induced ferroptosis and osteogenic dysfunction, supporting that Semaglutide preserves osteoblast function, at least in part, through suppression of Wnt5a signaling.

Activation of p38 MAPK Reverses the Inhibitory Effects of Semaglutide on Ferroptosis

To further confirm that the protective effect of semaglutide (SEMA) against HGHP-induced ferroptosis is mediated through the p38 MAPK signaling pathway, the specific p38 activator anisomycin was applied. As shown by ALP and Alizarin Red S staining, semaglutide markedly restored osteogenic differentiation and mineralization impaired under HGHP exposure, whereas co-treatment with anisomycin largely abolished these restorative effects (Figure 7A). Consistently, the mRNA and protein expression levels of osteogenic markers RUNX2, ALP, COL1, and OCN were significantly upregulated in the HGHP+SEMA group compared with HGHP alone, but were notably reduced following anisomycin addition (Figure 7B–D). These findings suggest that activation of p38 MAPK counteracts semaglutide-induced osteogenic recovery. Fluorescence staining further revealed that semaglutide markedly reduced lipid ROS accumulation, while anisomycin significantly reversed this reduction (Figure 7E and F). Moreover, semaglutide treatment substantially increased the expression of ferroptosis-suppressing proteins GPX4 and SLC7A11, indicating attenuation of ferroptotic injury, whereas anisomycin reversed these changes (Figure 7G and H). Correspondingly, semaglutide markedly inhibited phosphorylation of p38 and MAPK9, while anisomycin co-treatment reinstated their phosphorylation, confirming pathway reactivation (Figure 7I and J).

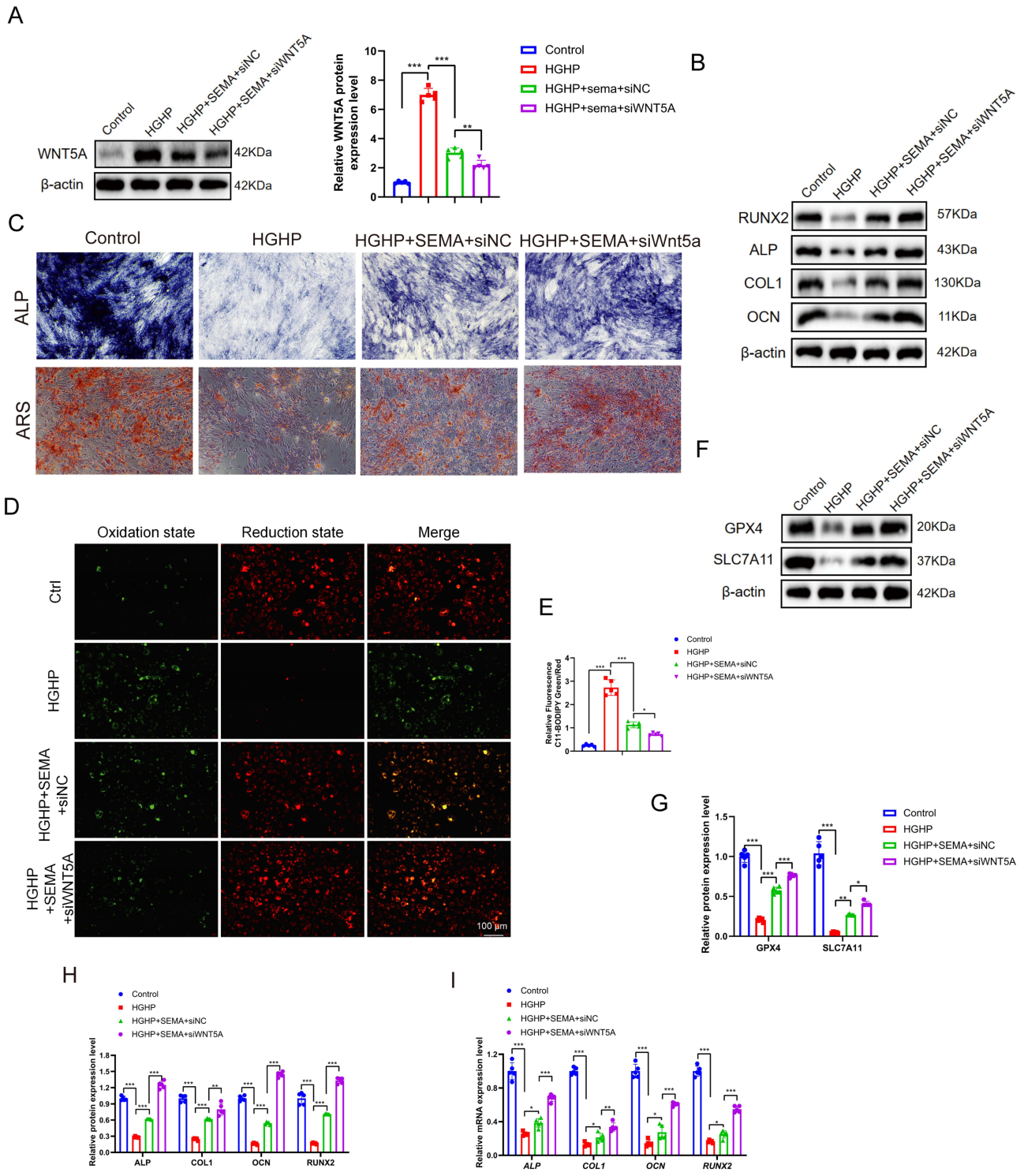

Figure 6 Wnt5a is required for the protective effects of semaglutide against HGHP-induced ferroptosis and osteogenic impairment. (**A**) Western blot analysis of Wnt5a expression and quantification of Wnt5a protein levels in osteoblasts under different treatment conditions (Ctronl, HGHP, HGHP+Sema+siNC, HGHP+Sema+siWnt5a). (**B**) Western blot analysis of osteogenic proteins (RUNX2, ALP, COL1, OCN). (**C**) ALP staining (day 7) and Alizarin Red S (ARS) staining (day 14) showing osteogenic differentiation. (**D**) Lipid ROS fluorescence staining in osteoblasts. (**E**) Quantitative analysis of lipid ROS levels. (**F**) Western blot analysis of ferroptosis-related proteins GPX4 and SLC7A11. (**G**) Densitometric quantification of ferroptosis-related proteins. (**H**) Western blot analysis of osteogenic proteins. (**I**) RT-qPCR analysis of osteogenic genes (RUNX2, ALP, COL1, OCN). Data are presented as mean ± SD (n = 5). *$P < 0.05$, **$P < 0.01$, ***$P < 0.001$. Scale bars = 100 μm.

https://doi.org/10.2147/DDDT.S599539

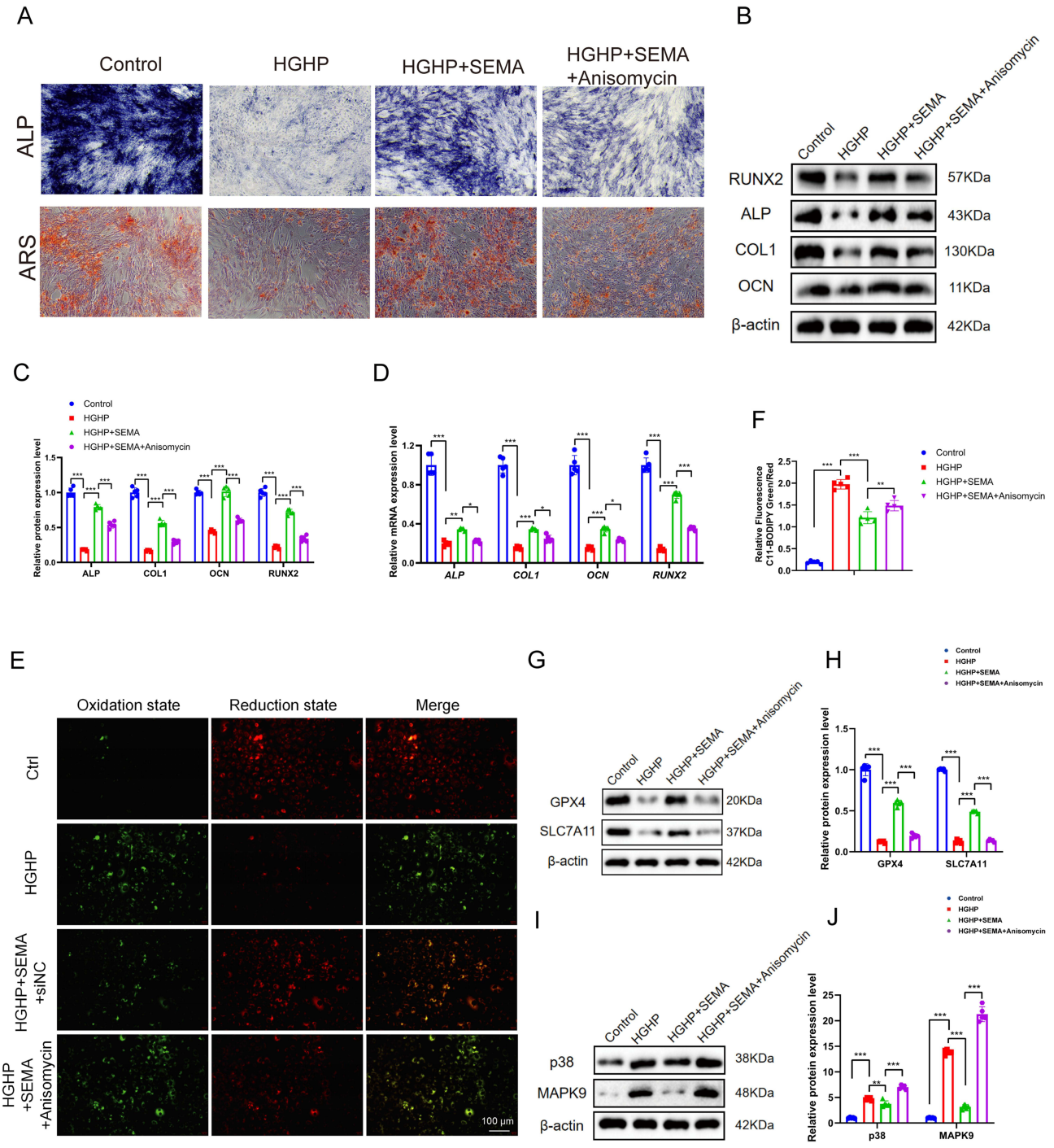

Figure 7 Activation of p38 MAPK reverses the inhibitory effects of semaglutide on ferroptosis in osteoblasts.(**A**) ALP staining (day 7) and Alizarin Red S (ARS) staining (day 14) showing osteogenic differentiation in different groups (Ctronl, HGHP, HGHP+SEMA, HGHP+SEMA+Anisomycin). (**B**) Western blot analysis of osteogenic proteins (RUNX2, ALP, COL1, OCN). (**C**) Densitometric quantification of osteogenic proteins. (**D**) RT-qPCR analysis of osteogenic genes (RUNX2, ALP, COL1, OCN). (**E**) Lipid ROS fluorescence staining. (**F**) Quantitative analysis of lipid ROS levels.(**G**) Western blot analysis of ferroptosis-related proteins GPX4 and SLC7A11. (**H**) Densitometric quantification of ferroptosis-related proteins. (**I**) Western blot analysis of phosphorylated p38 and MAPK9. (**J**) Densitometric quantification of phosphorylated p38 and MAPK9. Data are presented as mean ± SD (n = 5). **P < 0.05, **P < 0.01, ***P < 0.001* vs. *HGHP+SEMA group*. Scale bars = 100 μm.

Collectively, these results demonstrate that semaglutide mitigates ferroptosis and promotes osteogenic differentiation by suppressing the p38 MAPK signaling pathway, whereas pharmacological activation of p38 with anisomycin abolishes these beneficial effects.

https://doi.org/10.2147/DDDT.S599539

Semaglutide Ameliorates Periodontitis and Reduces Ferroptosis in a Type 2 Diabetic Mouse Model

To further investigate the in vivo effects of semaglutide on ferroptosis and periodontal tissue remodeling under diabetic conditions, a type 2 diabetic (T2DM) mouse model was established through high-fat/high-glucose feeding combined with streptozotocin (STZ) injection. Experimental periodontitis was induced by ligating the maxillary molars, and mice were divided into five groups: control, T2DM, diabetic periodontitis (DP), DP+Semaglutide (0.5 mg/kg), and DP+Fer-1 (1.5 mg/kg). The overall experimental design and treatment protocol are illustrated in Figure 8A. Histological examination by H&E staining showed that the DP group exhibited extensive inflammatory infiltration, irregular bone crest morphology, and disrupted periodontal ligament structure, while semaglutide markedly preserved alveolar bone height and reduced inflammatory damage (Figure 8B). Immunohistochemical analysis revealed that the expression of GPX4 was significantly decreased and OPN was elevated in DP mice, reflecting impaired osteogenic function and enhanced ferroptotic activity. Semaglutide administration restored GPX4 expression and reduced OPN levels, indicating inhibition of ferroptosis and improvement of osteogenic capacity in vivo (Figure 8C). Immunofluorescence staining demonstrated a strong positive signal of 4-HNE, a marker of lipid peroxidation and ferroptosis, in the periodontal tissues of DP mice. Notably, semaglutide and Fer-1 treatments both reduced 4-HNE accumulation (Figure 8D). Quantitative analysis further confirmed the changes in GPX4, OPN, and 4-HNE expression levels (Figure 8E).

Collectively, these findings confirm that semaglutide effectively alleviates alveolar bone loss and periodontal inflammation in diabetic mice, primarily by suppressing ferroptosis and restoring bone-forming potential.

Discussion

In this study, we explored the role of Semaglutide (SEMA) in modulating osteoblast ferroptosis and osteogenic dysfunction under diabetic conditions, and elucidated the underlying molecular mechanisms. Our results demonstrated that Semaglutide significantly alleviated high glucose and high palmitate (HGHP)-induced ferroptotic injury and restored osteogenic capacity in MC3T3-E1 cells. Mechanistically, Semaglutide exerted these effects through inhibition of the Wnt5a/Ror2/p38 MAPK signaling pathway, thereby suppressing oxidative stress and lipid peroxidation while enhancing osteogenic differentiation. Consistent with these findings, Semaglutide also ameliorated alveolar bone loss and restored bone remodeling in diabetic periodontitis (DP) mice. These findings suggest that Semaglutide confers bone-protective effects by targeting ferroptosis-related pathways in diabetic periodontitis.

The current study provides mechanistic insight into how ferroptosis contributes to osteoblast dysfunction in diabetic microenvironments.[8,12,23,24] Consistent with previous studies linking ferroptosis to periodontal tissue injury, fibroblast ferroptosis has been reported to contribute to periodontitis-induced tissue damage and alveolar bone loss, highlighting the pathological relevance of ferroptosis in periodontal disease.[5] Ferroptosis, a newly identified form of regulated cell death characterized by iron accumulation and lipid peroxidation, has been implicated in metabolic and inflammatory diseases.[11,12,23] Under HGHP conditions, osteoblasts displayed typical ferroptotic phenotypes, including increased ROS production, elevated Fe^{2+} levels, and decreased GPX4 and SLC7A11 expression, leading to impaired proliferation, migration, and mineralization. These results are consistent with previous reports showing that hyperglycemia and lipotoxicity trigger ferroptosis through disruption of redox homeostasis and mitochondrial integrity. Importantly, inhibition of ferroptosis by Ferrostatin-1 effectively reversed osteogenic impairment, confirming that ferroptosis is a major contributor to osteoblast dysfunction in diabetic periodontitis.

Our findings further demonstrated that Semaglutide effectively counteracted HGHP-induced osteoblast injury. Semaglutide treatment improved osteoblast proliferation and migration, enhanced alkaline phosphatase (ALP) activity and calcium deposition, and restored the expression of osteogenic markers RUNX2, COL1, and OCN. Meanwhile, Semaglutide reduced intracellular ROS and lipid peroxidation levels while upregulating GPX4 and SLC7A11, suggesting suppression of ferroptotic signaling. These protective effects are consistent with the known antioxidative and anti-inflammatory properties of GLP-1 receptor agonists. Interestingly, RNA sequencing and KEGG pathway enrichment analysis revealed that the Wnt5a/Ror2/p38 MAPK axis was significantly activated under HGHP stimulation but suppressed by Semaglutide treatment, indicating a potential mechanistic link between GLP-1R activation and Wnt-mediated ferroptotic signaling.[14–16]

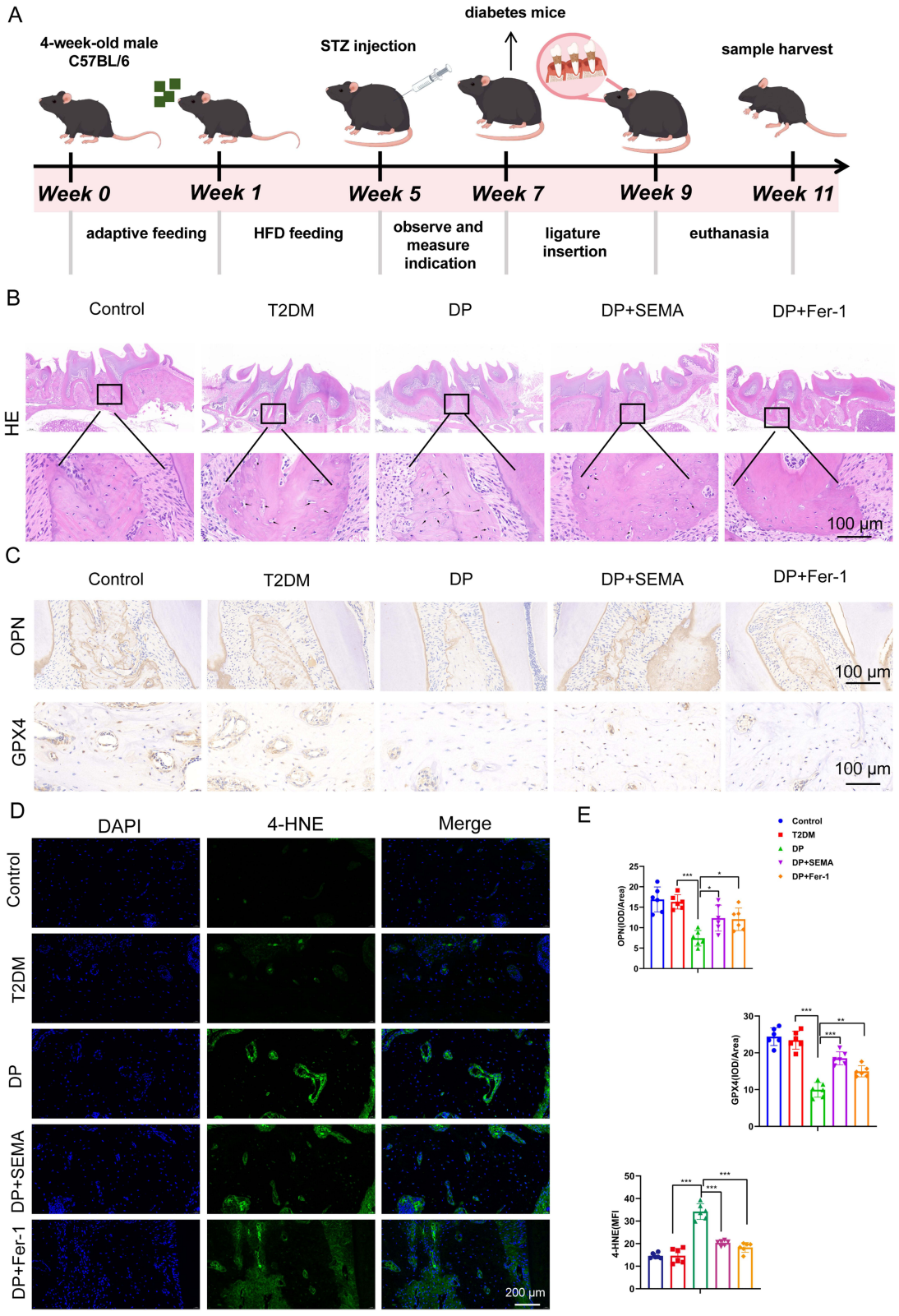

Figure 8 Semaglutide ameliorates periodontitis and suppresses ferroptosis in a type 2 diabetic mouse model. (**A**) Schematic diagram of the experimental design for the T2DM and diabetic periodontitis (DP) mouse model and treatment groups (Ctronl, T2DM, DP, DP+Sema 0.5 mg/kg, DP+Fer-1 1.5 mg/kg). (**B**) Hematoxylin and eosin (H&E) staining of periodontal tissues showing alveolar bone morphology and inflammatory infiltration. (**C**) Immunohistochemical staining of OPN and GPX4. (**D**) Immunofluorescence staining of 4-HNE indicating lipid peroxidation. (**E**) Quantitative analysis of GPX4, OPN, and 4-HNE expression. Data are presented as mean ± SD (n = 6). *$P < 0.05$, **$P < 0.01$, ***$P < 0.001$. Scale bars = 200 μm.

https://doi.org/10.2147/DDDT.S599539

To further validate this mechanism, we employed Wnt5a knockdown and p38 MAPK activation assays. Silencing Wnt5a reproduced the protective effects of Semaglutide, including improved osteogenic differentiation and reduced ferroptosis. In contrast, activation of p38 MAPK using Anisomycin reversed the anti-ferroptotic and pro-osteogenic effects of Semaglutide, confirming that Semaglutide acts upstream of Wnt5a/Ror2/p38 MAPK signaling. These findings are consistent with earlier studies indicating that Wnt5a-mediated noncanonical signaling promotes oxidative stress and inflammation in metabolic bone disorders. Therefore, our results establish that the inhibition of Wnt5a/Ror2/p38 MAPK signaling represents a key mechanism through which Semaglutide suppresses osteoblastic ferroptosis and restores bone-forming potential under diabetic conditions.

The in vivo experiments further substantiated our in vitro findings. In diabetic periodontitis mice, Immunohistochemical staining revealed enhanced expression of osteogenic proteins such as osteopontin (OPN) and decreased ferroptosis markers GPX4 and SLC7A11, supporting the notion that Semaglutide mitigates ferroptotic injury in periodontal bone tissue. Moreover, the therapeutic effects of Semaglutide were comparable to those of Ferrostatin-1, further indicating that its protective mechanism is closely associated with ferroptosis inhibition. Collectively, these results suggest that Semaglutide can serve as a potential pharmacological agent for preventing or treating diabetic bone loss by targeting ferroptotic pathways.

Taken together, this study provides strong evidence that Semaglutide attenuates osteoblast ferroptosis and restores osteogenic function through modulation of the Wnt5a/Ror2/p38 MAPK signaling pathway. This mechanistic insight extends the biological scope of GLP-1 receptor agonists beyond glucose regulation and highlights their potential role in maintaining skeletal homeostasis under metabolic stress. Given that Semaglutide is already approved for clinical use in diabetes and obesity, these findings open a promising avenue for its repurposing in diabetic periodontitis and other bone metabolic diseases.

Nevertheless, several limitations should be acknowledged. First, although our study revealed that Wnt5a/Ror2/p38 MAPK signaling mediates the protective effects of Semaglutide, potential cross-talk with other signaling pathways such as Nrf2/HO-1, NF-κB, or AMPK/mTOR cannot be excluded.[20] Second, our cellular experiments were conducted using MC3T3-E1 preosteoblastic cells;[25] thus, further studies employing primary human osteoblasts or periodontal stem cells are required to confirm translational relevance. Finally, the direct molecular interaction between GLP-1 receptor activation and Wnt5a expression remains to be elucidated, which warrants further investigation using molecular and genetic tools.

In conclusion, our findings demonstrate that Semaglutide suppresses osteoblastic ferroptosis and promotes osteogenic differentiation under diabetic conditions by inhibiting the Wnt5a/Ror2/p38 MAPK signaling pathway. This study provides novel insights into the protective mechanisms of GLP-1 receptor agonists in diabetic bone metabolism and suggests that targeting ferroptosis may represent a new therapeutic approach for diabetic periodontitis and related skeletal disorders.

Conclusion

In summary, our study identifies ferroptosis as a critical mediator of osteogenic impairment in diabetic periodontitis and demonstrates that Semaglutide mitigates ferroptosis and restores bone formation by modulating the Wnt5a/Ror2/p38 MAPK pathway. These findings provide new mechanistic insight into GLP-1RA-mediated bone protection and suggest a promising therapeutic approach for preventing diabetic bone loss.

Author Contributions

Zhenzhang contributed to conceptualization, methodology, formal analysis, validation, visualization, and writing – original draft. Delong Niu contributed to conceptualization and validation. Wenjie Qiu contributed to methodology and validation. Haoyu Feng contributed to formal analysis and validation. Lurong Jia contributed to writing – review and editing and project administration. Wenjuanzhou contributed to conceptualization, methodology, supervision, funding acquisition, and writing – review and editing. All authors made a significant contribution to the work reported, including study design, data acquisition, analysis, and interpretation; participated in drafting, revising, or critically reviewing the article; approved the final version to be published; agreed on the journal to which the article has been submitted; and agreed to be accountable for all aspects of the work.

Funding

This study was supported by the National Natural Science Foundation of China,Grant number [82201110].

Disclosure

The authors declare no competing interests.

References

1. Lalla E, Papapanou PN. Diabetes mellitus and periodontitis: a tale of two common interrelated diseases. *Nat Rev Endocrinol*. 2011;7(12):738–748. doi:10.1038/nrendo.2011.106
2. Polak D, Shapira L. An update on the evidence for pathogenic mechanisms that may link periodontitis and diabetes. *J Clin Periodontol*. 2018;45 (2):150–166. doi:10.1111/jcpe.12803
3. Dixon SJ, Lemberg KM, Lamprecht MR, et al. Ferroptosis: an iron-dependent form of nonapoptotic cell death. *Cell*. 2012;149(5):1060–1072.
4. Stockwell BR, Angeli JP, Bayir H, et al. Ferroptosis: a regulated cell death nexus linking metabolism, redox biology, and disease. *Nat Rev Cell Biol*. 2017;19(5):267–285.
5. Xing L, Dong W, Chen Y, et al. Fibroblast ferroptosis is involved in periodontitis-induced tissue damage and bone loss. *Int Immunopharmacol*. 2023;114:109607. doi:10.1016/j.intimp.2022.109607
6. Fang X, et al. Ferroptosis as a target for protection against cardiovascular and neurodegenerative diseases. *Nat Rev Drug Discov*. 2023;22 (8):611–632.
7. Lu S, et al. Ferroptosis and bone homeostasis: molecular mechanisms and therapeutic opportunities. *Bone Res*. 2024;12(1):21.
8. Yang R, Wang X, Krishnamoorthi S, et al. Ferroptosis promotes diabetic bone loss by impairing osteoblast differentiation. *Redox Biol*. 2022;51:102280. doi:10.1016/j.redox.2022.102280
9. Lin C, Khan MSS, Ahmed S, et al. Iron overload-induced ferroptosis contributes to periodontal tissue damage in diabetic rats. *Free Radic Biol Med*. 2023;204:82–94. doi:10.1016/j.freeradbiomed.2023.04.011
10. Tang D, et al. Ferroptosis: molecular mechanisms and health implications. *Signal Transduct Target Ther*. 2023;8(1):241. doi:10.1038/s41392-023-01514-4
11. Zhang Y, Zheng M, Ning Y, et al. Ferroptosis-related gene signatures in periodontitis: a bioinformatics analysis. *J Transl Med*. 2023;21(1):456. doi:10.1186/s12967-023-04284-3
12. Guo W, et al. Ferroptosis contributes to inflammatory alveolar bone loss in diabetes. *Front Immunol*. 2024;15:1412029.
13. Maeda K, et al. Wnt5a-Ror2 signaling regulates cell polarity and directional movement in osteoblasts. *Mol Cell Biol*. 2012;32(21):4225–4237.
14. Gao Y, et al. Wnt5a promotes inflammatory responses in periodontitis via activation of JNK and p38. *J Clin Periodontol*. 2022;49(4):380–392.
15. Kim JH, et al. Wnt5a induces osteoclastogenesis by regulating LPS-mediated inflammatory responses. *J Biol Chem*. 2018;293(11):4449–4461.
16. Baron R, Kneissel M. WNT signaling in bone homeostasis and disease: from human mutations to treatments. *Nat Med*. 2013;19(2):179–192. doi:10.1038/nm.3074
17. Aoyama E, et al. Expression of glucagon-like peptide-1 receptor and its role in osteoblast proliferation. *Endocrinology*. 2014;155(2):357–367.
18. Jeon YK, et al. Glucagon-like peptide-1 receptor agonist promotes osteogenic differentiation of MC3T3-E1cells. *Mol Med Rep*. 2014;9 (5):1699–1706.
19. Rubino DM, et al. Effect of semaglutide on cardiovascular outcomes in patients with type 2 diabetes. *N Engl J Med*. 2021;385(17):1529–1539.
20. Anam AK, et al. Semaglutide and its pleiotropic effects: beyond glycemic control. *Nat Rev Endocrinol*. 2022;18(8):475–489.
21. Ma X, Sun Z, Li B, et al. GLP-1 receptor signaling promotes bone formation through modulation of oxidative stress. *Endocrinology*. 2023;164(4): bqad012. doi:10.1210/endocr/bqad012
22. Lv S, et al. GLP-1 receptor agonists improve bone metabolism by suppressing oxidative stress and inflammation. *Front Pharmacol*. 2023;14:1120238.
23. Ru Q, et al. Ferroptosis in metabolic bone diseases: mechanisms and therapeutic targets. *Front Cell Dev Biol*. 2023;11:1162047.
24. Lin Y, Shen X, Ke Y, et al. Activation of osteoblast ferroptosis via the METTL3/ASK1-p38 signaling pathway in high glucose and high fat (HGHF)-induced diabetic bone loss. *FASEB j*. 2022;36(3):e22147. doi:10.1096/fj.202101610R
25. Czekanska EM, Stoddart MJ, Richards RG, et al. In search of an osteoblast cell model for in vitro research. *Eur Cell Mater*. 2012;24:1–17. doi:10.22203/eCM.v024a01